Metadata of the chapter that will be visualized online

Chapter Title	Pseudoelasticity and Shape Memory Effect: A Maxwellian Rate-Type Approach	
Copyright Year	2013	
Copyright Holder	Springer Science+Business Media Dordrecht	
Corresponding Author	Family Name	**Făciu**
	Particle	
	Given Name	**Cristian**
	Suffix	
	Organization/University	“Simion Stoilow” Institute of Mathematics of the Romanian Academy, Research Unit No. 6
	Postbox	1-764
	Postcode	014700
	City	Bucharest
	Country	Romania
	Phone	00 40 21 319 65 06
	Fax	00 40 21 319 65 05
	Email	Cristian.Faciu@imar.ro

P

Pseudoelasticity and Shape Memory Effect: A Maxwellian Rate-Type Approach

Cristian Făciu
"Simion Stoilow" Institute of Mathematics of the Romanian Academy, Research Unit No. 6, Bucharest, Romania

Overview

The pseudoelasticity and the shape memory effect are two fundamental aspects of the thermomechanical behavior of shape memory alloys (SMA) (see [1]). These remarkable properties are due to a solid-solid phase transformation from austenite to martensite and back again. The phase transformation occurs through the nucleation and propagation of phase transformation fronts. These events lead to distinctly nonuniform deformation and temperature fields. Local to each transformation front is the generation or absorption of latent heat which can cause self-heating or self-cooling of the material. One considers a Maxwellian rate-type constitutive equation which combines the thermodynamic properties of the thermoelastic materials analyzed in ▶ Thermoelastic Bar Theory with the rate-type effects described in ▶ Maxwellian Rate-Type Thermo-viscoelastic Bar Theory. It is shown that this thermomechanical continuum model has the capability to describe the strong thermomechanical coupling in the material behavior of SMA bars (pseudoelastic behavior in the isothermal case has been considered the first time in [2] while the non-isothermal case in [3]). The equilibrium set of the Maxwellian model can be derived from very low quasi-static uniaxial experiments of SMA bars. These laboratory experiments justify the need to consider non-monotone stress-strain curves at constant temperature. The temperature dependence of the stress-strain relation is determined from the experimental behavior of the hysteresis. The way the material behaves outside the equilibrium set is ruled by the rate-type effects of the Maxwellian constitutive relation which introduce a dissipative regularizing term allowing to describe stress relaxation phenomena toward equilibrium between phases. Its advantage is that no additional kinetic relation or nucleation criterion needs to be prescribed as in [4]. The nucleation of phases and their front propagation is automatically accounted for this model. The system of PDE which governs the motion leads to well-posed problem. The numerical simulations of the pseudoelastic response and of the shape memory effect show close qualitative agreement with previously reported experimental data.

R. Hetnarski (ed.), *Encyclopedia of Thermal Stresses*, DOI 10.1007/978-94-007-2739-7,

Shape Memory Alloys: Thermomechanical Aspects

SMAs are a unique group of alloys which shows two uncommon capabilities: the pseudoelasticity and the shape memory effect. *Pseudoelasticity* refers to the ability of the material in a certain regime of temperature to attain large mechanically induced strains (up to 8–10 %) during loading and then recover upon unloading via a hysteresis loop (Fig. 1a). The way the hysteresis loop moves downward as the temperature decreases is illustrated in Fig. 1 at two representative temperatures $\theta_1 > \theta_2$. The temperature range between θ_1 and θ_2 is typically 50°C around room temperature. The *shape memory effect*, illustrated in Fig. 1b, is the material's ability to recover, at a free-stress state, large strains induced mechanically, at the lower temperature θ_2, by a moderate increase in temperature ($\approx 10 - 20$°C) of the specimen.

The underlying mechanism is a reversible solid-solid phase transformation process from a crystallographically more ordered parent phase (austenite) to a crystallographically less ordered product phase (martensite). At high temperatures the alloy is in the highly symmetric stable phase austenite $\mathcal{A}$, while at low temperatures, the less symmetric phase martensite prevails. The martensite exists in twins. Under uniaxial loading conditions, one sees only two twins (or variants): one obtained for sufficiently large compressive strain and is denoted $\mathcal{M}^-$ and the other obtained for sufficiently large tensile strain and is denoted $\mathcal{M}^+$. The austenite may be called the low strain phase since it exists for small values of strain. We use in the following the terminology "three phases" rather than "one phase and two variants." For certain interval of temperature, the three phases can coexist and can transform from one to the other. The transformation can be induced by changes in temperature or by changes in stress due to the strong thermomechanical coupling in the material behavior.

The transformation from austenite to martensite and back again during the pseudoelastic response occurs through the nucleation and propagation of phase transformation fronts along the plateaus of the hysteresis. These events lead to distinctly nonuniform deformation and temperature fields. Local to each transformation front is the generation or absorption of latent heat which can cause self-heating during $\mathcal{A} \to \mathcal{M}^+$ transformation or self-cooling during reverse $\mathcal{M}^+ \to \mathcal{A}$ transformation of the material. All these properties make SMAs to be a class of materials with the ability to remember shape, by mechanical or thermal loading conditions, even after quite severe deformations. That explains why SMAs became an attractive choice for innovative structural applications (see [1, 5]).

To bridge the gap between microscopic structure and a macroscopic constitutive model is a complex task and constitutes an area of intensive research. The last decades have seen a variety of constitutive modeling efforts including purely phenomenological approaches, plasticity analogues, thermodynamically based continuum models, and detailed micromechanical models (see [1, 6], and their references).

We present in what follows a simple one-dimensional model which combines the Maxwellian rate-type effects with the thermodynamic properties of classical thermoelasticity with non-monotone stress-strain relations (see ▶ Maxwellian Rate-Type Thermo-viscoelastic Bar Theory). One shows that this approach can capture the thermomechanical coupling of the localized phase transformations that occurs during the response of SMA bars.

A Thermomechanical Continuum Model for SMAs Bars

Three-Phase Materials: Thermoelastic Equilibrium

Starting with the seminal paper by Ericksen [7], the reversible phase transformations in

crystalline solids have been successfully studied using the theory of thermoelasticity with non-monotone stress-strain relations, or non-convex free energy functions, for certain interval of temperature (see, for instance, [6] and the references). Let us consider such a stress-strain-temperature relation

$$\sigma = \sigma_{eq}(\varepsilon, \theta) \tag{1}$$

to describe the response of a SMA bar in tension and compression tests.

Information about this phenomenological constitutive relation can be derived from isothermal stress-strain curves obtained experimentally at low strain rates over an interval of temperature and from the macroscopic manifestations of the instability phenomena which accompany the phase transformation process. A typical example is given by the pseudoelastic response of a nearly equiatomic polycrystalline NiTi alloy under uniaxial traction strain-controlled tests reported in [8, Fig. 3] for temperatures between 15°C and 55°C (see also [9]). These experiments show a hysteretic behavior like in Fig. 1a with the following characteristics. The bar, initially in the low strain phase (austenite), starts to deform elastically in a homogeneous manner. This homogeneity is lost shortly after the maximum stress $\sigma_M^+ = \sigma_M^+(\theta)$, which corresponds to the strain level $\varepsilon_M^+ = \varepsilon_M^+(\theta)$, is reached. A significant stress drop accompanies the first nucleation of martensite, and the $\mathcal{A} \to \mathcal{M}^+$ phase transformation produces a well-defined upper stress plateau with small serrations. These oscillations represent the manifestation of the thermomechanical instability phenomena, which occur through the nucleation and propagation of phase transformation fronts. At the end of the plateau, the transformation is complete and the bar, in the martensite phase, starts again to deform elastically and homogeneously while the slope of the stress-strain relation is again positive.

During unloading the specimen deforms homogeneously in the new martensite phase $\mathcal{M}^+$. This homogeneity is lost shortly after a minimum stress $\sigma_m^+ = \sigma_m^+(\theta)$ has been reached (Fig. 1a), which corresponds to the strain $\varepsilon_m^+ = \varepsilon_m^+(\theta)$. After a sudden rise of the stress, unstable reverse $\mathcal{M}^+ \to \mathcal{A}$ transformation proceeds along a lower stress plateau by propagation of distinct phase fronts along the length of the unloaded specimen until the transformation is complete.

Along the loading and unloading stress plateaus, the two phases coexist. Moreover, coexistent phase distributions are possible for a single-axial stress state in the static case, that is, when we stop, for example, the loading conditions. This behavior requires to consider a non-monotone stress-strain relation, with a negative slope for the interval $(\varepsilon_M^+(\theta), \varepsilon_m^+(\theta))$. The assumption is in agreement with the usual association of the monotone increasing/decreasing stress-strain relation with the so-called stable/unstable states of the material.

The monotone increasing parts of the stress-strain isotherms can be chosen in such a way to fit quasi-static experimental results of the type illustrated in [8, Fig. 3]. On the other side, the monotone decreasing part of these curves cannot be determined in a direct way from such experiments. Consequently, in general, they are chosen in a conventional way. For simplicity one may choose a straight line which connects $(\varepsilon_M^+(\theta), \sigma_M^+(\theta))$ and $(\varepsilon_m^+(\theta), \sigma_m^+(\theta))$. It will be seen later that, for theories like those developed here, which include rate effects, the magnitude of the negative slope $\frac{\partial \sigma_{eq}(\varepsilon,\theta)}{\partial \varepsilon}$ affects only the kinetics of phase transformation, that is, the rate at which the transformation takes place. Indeed, it was shown in [10, Part II, Sect. 2] how the slope of the equilibrium curve influences the growth/decay of a perturbation of an equilibrium state.

In compression tests one observes the same characteristics of the hysteretic deformation, and we associate the minus sign to the compressive states which we introduce. What can be determined experimentally (see [9]) is the temperature dependence of the pairs $(\varepsilon_M^{\pm}(\theta), \sigma_M^{\pm}(\theta))$ and $(\varepsilon_m^{\pm}(\theta), \sigma_m^{\pm}(\theta))$, where the equilibrium stress-strain relation at constant temperature attains its local maxima and minima. Moreover, one observes that, for a three-phase material, there are two critical temperatures θ_m and θ_M, such as for $\theta > \theta_M$, the material only exists in its austenite form no matter what the stress level is, whereas for $\theta < \theta_m$, the material only exists in its martensitic variants. For $\theta \in (\theta_m, \theta_M)$ all three phases are available to the material. By combining this information, one can plot a phase diagram in the $\theta - \varepsilon$ plane of the type in Fig. 2a which contains essential constitutive information on phase transformation and allows to characterize the thermoelastic response function $\sigma = \sigma_{eq}(\varepsilon, \theta)$ for a three-phase material.

The above physical observations on the behavior of SMA bars in tension and compression tests result in considering a thermoelastic response function $\sigma = \sigma_{eq}(\varepsilon, \theta)$ with the following properties:

(a) At each temperature $\theta > \theta_M$, the stress response function $\sigma = \sigma_{eq}(\varepsilon, \theta)$ is a monotonically *increasing* function of strain.
(b) At each temperature $\theta \in (\theta_m, \theta_M)$, the stress response function $\sigma = \sigma_{eq}(\varepsilon, \theta)$ is a monotonically *increasing* function of strain for $\varepsilon < \varepsilon_m^-(\theta)$, for $\varepsilon \in (\varepsilon_M^-(\theta), \varepsilon_M^+(\theta))$, and for $\varepsilon > \varepsilon_m^+(\theta)$, and it is a monotonically *decreasing* function of strain over the intervals $(\varepsilon_m^-(\theta), \varepsilon_M^-(\theta))$ and $(\varepsilon_M^+(\theta), \varepsilon_m^+(\theta))$.
(c) At each temperature $\theta < \theta_m$, the stress response function $\sigma = \sigma_{eq}(\varepsilon, \theta)$ is a monotonically *increasing* function of strain for $\varepsilon < \varepsilon_m^-(\theta)$ and $\varepsilon > \varepsilon_m^+(\theta)$, while on the remaining interval $(\varepsilon_m^-(\theta), \varepsilon_m^+(\theta))$, it is monotonically *decreasing*.

In general, the boundary curves $\varepsilon = \varepsilon_M^{\pm}(\theta)$ and $\varepsilon = \varepsilon_m^{\pm}(\theta)$ fix the limits of the regions in the $\theta - \varepsilon$ plane on which the austenite phase A and the martensite variants $\mathcal{M}^{\pm}$ exist, while their images through the function $\sigma = \sigma_{eq}(\varepsilon, \theta)$ onto the plane $\sigma - \theta$ bound the regions which describe the phases that are available to a particle at a given (σ, θ) (see Fig. 2).

The dependence of the stress response function $\sigma = \sigma_{eq}(\varepsilon, \theta)$ on temperature should reflect the fact that in traction tests [8], the hysteresis loop moves *upward*, while in compression tests, it moves *downward*, as the temperature grows. That means:

(d) There exists a monotone curve $\varepsilon = \varepsilon_t(\theta) \in (\varepsilon_M^-(\theta), \varepsilon_M^+(\theta))$ such that $\frac{\partial \sigma_{eq}(\varepsilon,\theta)}{\partial \theta} > 0$, for $\varepsilon > \varepsilon_t(\theta)$ and $\frac{\partial \sigma_{eq}(\varepsilon,\theta)}{\partial \theta} < 0$, for $\varepsilon < \varepsilon_t(\theta)$.

It is this property which allows to the model to describe the *exothermic* character of $\mathcal{A} \to \mathcal{M}^{\pm}$ phase transformation and the *endothermic* character of $\mathcal{M}^{\pm} \to \mathcal{A}$.

An Explicit Piecewise Linear Thermoelastic Model

Experiments on SMAs show that a material in a pure phase has in general a linear thermoelastic behavior. Therefore, we can assume that the elastic moduli of the austenite phase $\mathcal{A}$ and martensite variants $\mathcal{M}^{\pm}$ are constant and equal to $E_1 > 0$ and $E_3 > 0$, respectively. Moreover, we suppose that the elastic moduli of the (unstable) regions, defined as $\mathcal{I}^- = \{(\varepsilon, \theta) | \varepsilon \in (\varepsilon_m^-(\theta), \varepsilon_M^-(\theta))\}$ and $\mathcal{I}^+ = \{(\varepsilon, \theta) | \varepsilon \in (\varepsilon_M^+(\theta), \varepsilon_m^+(\theta))\}$, are also constant and equal to $-E_2 < 0$ (Fig. 2).

Therefore, one derives the following expression of the thermoelastic equilibrium for $\theta \in (\theta_m, \theta_M)$:

$$\sigma_{eq}(\varepsilon,\theta)=\begin{cases} E_3(\varepsilon-\varepsilon_m^-(\theta))+\sigma_m^-(\theta) & \text{if} \quad \varepsilon\le\varepsilon_m^-(\theta)\\ -E_2(\varepsilon-\varepsilon_m^-(\theta))+\sigma_m^-(\theta) & \text{if } \varepsilon_m^-(\theta)<\varepsilon<\varepsilon_M^-(\theta)\\ E_1(\varepsilon-\varepsilon_M^-(\theta))+\sigma_M^-(\theta) & \text{if } \varepsilon_M^-(\theta)\le\varepsilon\le\varepsilon_M^+(\theta)\\ -E_2(\varepsilon-\varepsilon_M^+(\theta))+\sigma_M^+(\theta) & \text{if } \varepsilon_M^+(\theta)<\varepsilon<\varepsilon_m^+(\theta)\\ E_3(\varepsilon-\varepsilon_m^+(\theta))+\sigma_m^+(\theta) & \text{if } \varepsilon_m^+(\theta)\le\varepsilon \end{cases} \tag{2}$$

In order to describe a linear thermoelastic behavior in a pure phase, one supposes that the constitutive functions $\varepsilon_M^{\pm}(\theta)$ and $\varepsilon_m^{\pm}(\theta)$ are linear. One derives in [3] using some ideas from [4] the following explicit form:

$$\begin{aligned}\varepsilon_M^{\pm}(\theta)&=\alpha(\theta-\theta_T)\pm M(\theta-\theta_m)\\ \varepsilon_m^{\pm}(\theta)&=\alpha(\theta-\theta_T)\mp(M-m)(\theta-\theta_M)\pm M(\theta-\theta_m)\end{aligned} \tag{3}$$

while for $\sigma_M^{\pm}(\theta)=\sigma_{eq}(\varepsilon_M^{\pm}(\theta),\theta)$ and $\sigma_m^{\pm}(\theta)=\sigma_{eq}(\varepsilon_m^{\pm}(\theta),\theta)$, the local maxima and minima with respect to ε of the stress-strain relation at constant temperature, we have

$$\begin{aligned}\sigma_M^{\pm}(\theta)&=\pm E_1M(\theta-\theta_m),\\ \sigma_m^{\pm}(\theta)&=\pm E_2(M-m)(\theta-\theta_M)\pm E_1M(\theta-\theta_m)\end{aligned} \tag{4}$$

Since the stress response function in $\mathcal{A}$ phase becomes $\sigma_{eq}(\varepsilon,\theta)=E_1\varepsilon-E_1\alpha(\theta-\theta_T)$, it is obvious that $\alpha=\text{const.}>0$ is the thermal expansion coefficient of the material in this phase and θ_T is a reference temperature such that the undeformed material is stress free in the austenite phase, that is, $\sigma_{eq}(0,\theta_T)=0$. According to [9], the quantities $\frac{\mathrm{d}\sigma_M^+(\theta)}{\mathrm{d}\theta}$ and $\frac{\mathrm{d}\sigma_m^+(\theta)}{\mathrm{d}\theta}$ can be determined experimentally. That allows to identify the two positive material constants M and m.

One considers a hypothetical model characterized by the following constants:

$$\begin{aligned}&E_1=30.\,\text{GPa},\ E_2=0.5\,\text{GPa},\ E_3=20.5\,\text{GPa},\\ &\alpha=1.6^{-6}/^{\circ}\text{K},\ \theta_T=283.15\,^{\circ}\text{K},\\ &\theta_m=280\,^{\circ}\text{K},\ \theta_M=10,000\,^{\circ}\text{K},\\ &M=10.1371^{-5}/^{\circ}\text{K},\ m=9.7253^{-5}/^{\circ}\text{K}.\end{aligned} \tag{5}$$

For these numerical entries, Fig. 3a shows the evolution of the piecewise linear isotherms given by (2) with respect to the temperature.

The free energy function of the thermoelastic model (see ▶ Thermoelastic Bar Theory) is given by $\varrho\psi_{eq}(\varepsilon,\theta)=\int_0^{\varepsilon}\sigma_{eq}(s,\theta)\mathrm{d}s+\varrho\phi(\theta)$, where ϱ is the mass density and function $\phi=\phi(\theta)$ is solution of the equation $-\theta\frac{\mathrm{d}^2\phi(\theta)}{\mathrm{d}\theta^2}=C$. Here, $C=\text{const.}$ represents the specific heat at constant strain in the austenite phase. The free energy is illustrated in Fig. 3b for $C=500\,\text{J/Kg}/^{\circ}\text{C}$, $\varrho=8000\,\text{kg/m}^3$, and input data (5). One sees that $\psi=\psi_{eq}(\varepsilon,\theta)$ is convex in ε if $\frac{\partial\sigma_{eq}(\varepsilon,\theta)}{\partial\varepsilon}>0$, and it is concave in ε if $\frac{\partial\sigma_{eq}(\varepsilon,\theta)}{\partial\varepsilon}<0$, for fixed θ.

The adiabatic sound speed $U(\varepsilon,\theta)$ or, equivalently, the characteristic directions of the adiabatic thermoelastic system are real solutions of the equation $\varrho U^2(\varepsilon,\theta)=\frac{\partial\sigma_{eq}}{\partial\varepsilon}+\frac{\theta}{\varrho C_{eq}}\left(\frac{\partial\sigma_{eq}}{\partial\theta}\right)^2$ (see ▶ Thermoelastic Bar Theory). One can notice that for the stress response function (2) and the input data (5), the regions $\mathcal{A}=\left\{(\varepsilon,\theta)|\varepsilon\in(\varepsilon_{\mathcal{M}}^-(\theta),\varepsilon_{\mathcal{M}}^+(\theta))\right\}$, $\mathcal{M}^+=\left\{(\varepsilon,\theta)|\varepsilon>\varepsilon_m^+(\theta)\right\}$, and $\mathcal{M}^-=\{(\varepsilon,\theta)|\varepsilon<\varepsilon_m^-(\theta)\}$ correspond to the domains where the adiabatic sound speed is real, that is, to the domains of hyperbolicity of the adiabatic thermoelastic system. Unlike these, the domains $\mathcal{I}^{\pm}$ correspond to the domains of ellipticity. Thus, one identifies the stable phases of the material $\mathcal{A}$ and $\mathcal{M}^{\pm}$ with the domains of hyperbolicity of the adiabatic thermoelastic system, while the unstable phases $\mathcal{I}^{\pm}$ with the domains of ellipticity.

This change of type of the system leads to mathematical ill-posed problems. Therefore, by using only the thermoelastic model (2), one cannot describe the transition process between two stable phases. That is due to a lack of constitutive information.

A usual way to remedy this deficiency (see, e.g., [6] and the references therein) is to add two notions from material sciences in the continuum setting: a nucleation criterion for the initiation of phase transition and a kinetic relation between interface velocity and the driving force of phase transformation. A different way, which we consider in the following, is to augment the thermoelastic theory by incorporating rate effects.

A Maxwellian Rate-Type Approach

One considers that the stress depends not only on strain and temperature through the equilibrium relation $\sigma_{eq}(\varepsilon,\theta)$ but also on the strain rate and the stress rate. A dissipative mechanism, which is missing in a pure thermoelastic approach, is introduced through the following Maxwellian rate-type constitutive equation (see ▶ Maxwellian Rate-Type Thermo-viscoelastic Bar Theory):

$$\frac{\partial\sigma}{\partial t}-E\frac{\partial\varepsilon}{\partial t}=-\frac{E}{\mu}(\sigma-\sigma_{eq}(\varepsilon,\theta)), \tag{6}$$

where $E=\text{const.}>0$ is called the dynamic Young modulus and $\mu=\text{const.}>0$ is a Newtonian viscosity coefficient. $\frac{\mu}{E}$ is a relaxation time of the material, while $k=\frac{E}{\mu}$ is called the Maxwellian viscosity coefficient. This relaxation time should be related with a phase transition time characterizing the time needed to a particle to cross the unstable regions $\mathcal{I}^{\pm}$.

It was proved that the existence of a unique free energy $\psi_{mx}=\psi_{mx}(\varepsilon,\sigma,\theta)$, entropy $\eta_{mx}=\eta_{mx}(\varepsilon,\sigma,\theta)=-\frac{\partial\psi_{mx}}{\partial\theta}$, and a positive specific heat $C_{mx}=-\theta\frac{\partial^2\psi_{mx}}{\partial\theta^2}$, compatible with the second law of thermodynamics, is ensured if and only if the constitutive functions satisfy the subcharacteristic condition $U^2=\frac{\partial\sigma_{eq}}{\partial\varepsilon}+\frac{\theta}{\varrho C_{eq}}\left(\frac{\partial\sigma_{eq}}{\partial\theta}\right)^2<E$. Moreover, it has been shown that the free energy function $\psi_{mx}=\psi_{mx}(\varepsilon,\sigma,\theta)$ is uniquely determined (modulo an additive function of temperature) by the equilibrium states described by $\sigma_{eq}(\varepsilon,\theta)$ and by the dynamic Young modulus E. The additive function can be determined by knowing the specific heat at a constant strain over an interval of temperature $C_{eq}(\varepsilon_0,\theta)$ for the thermoelastic model.

Field Equations

We consider a thin bar of circular cross-sectional area of radius R and length L in a reference configuration. The field quantities are uniform over a cross section, that is, they only depend on (X,t) where $t>0$ is the time and $X\in[0,L]$ is the initial coordinate. According to the thermomechanical bar theory in Lagrangian description (see ▶ Thermoelastic Bar Theory) and to the thermodynamical properties of Maxwellian rate-type constitutive equation (see ▶ Maxwellian Rate-Type Thermo-viscoelastic Bar Theory), the governing system of equations consists of the balance law of momentum, the compatibility condition between the particle velocity v and the strain ε, the rate-type constitutive equation, and the balance of energy:

$$\varrho\frac{\partial v}{\partial t}=\frac{\partial\sigma}{\partial X}, \tag{7}$$

$$\frac{\partial\varepsilon}{\partial t}=\frac{\partial v}{\partial X} \tag{8}$$

$$\frac{\partial\sigma}{\partial t}-E\frac{\partial\varepsilon}{\partial t}=G(\varepsilon,\sigma,\theta)\overset{\text{def}}{=}-\frac{E}{\mu}(\sigma-\sigma_{eq}(\varepsilon,\theta) \tag{9}$$

$$\varrho C_{mx}\frac{\partial\theta}{\partial t}=-\varrho\frac{\partial\psi_{mx}}{\partial\sigma}G(\varepsilon,\sigma,\theta)+\varrho\theta\frac{\partial^2\psi_{mx}}{\partial\sigma\partial\theta}G(\varepsilon,\sigma,\theta)+\kappa\frac{\partial^2\theta}{\partial X^2}-\frac{2\omega}{R}(\theta-\theta_{ext}(t)), \tag{10}$$

where $\kappa>0$ is the Fourier heat conductivity coefficient, $\omega>0$ is a material parameter characterizing the heat exchanges across the lateral surface of the bar with its environment, and $\theta_{ext}(t)$ is the uniform temperature of the surroundings at time t.

The first term in the right part of (10) is always positive and represents the heating due to the

internal dissipation. The second term represents the heating or the cooling due to the latent heat absorbed or released by the body during a phase transformation process. It strongly depends on $\frac{\partial \sigma_{eq}}{\partial \theta}$, and its contribution is dominant with respect to the internal dissipation. The last term gives account on the gain or loss of heat across the lateral surface of the bar.

In the absence of axial heat conduction, that is, when $\kappa = 0$, the system is always hyperbolic semilinear with sources (see ▶ Maxwellian Rate-Type Thermo-viscoelastic Bar Theory). The first two sources are stiff since the time of relaxation $\frac{\mu}{E}$ is very small. If the axial conduction is taken into account, then the system is of hyperbolic-parabolic type. In both cases the initial-boundary value problems are well posed irrespective of the sign of $\frac{\partial \sigma_{eq}}{\partial \varepsilon}$, hence, even in the unstable regions $\mathcal{I}^{\pm}$. Consequently, the system is appropriate to describe the process of phase transition between the stable phases $\mathcal{A}$ and $\mathcal{M}^{\pm}$.

If one investigates the local behavior of the solutions of the Maxwellian rate-type system (7)–(10), that is, one performs a linear stability analysis of a perturbation of an equilibrium state satisfying $\sigma_0 = \sigma_{eq}(\varepsilon_0, \theta_0)$, one gets (a) an exponential growth in time of the perturbation if $\frac{\partial \sigma_{eq}(\varepsilon_0,\theta_0)}{\partial \varepsilon} < 0$ which causes material instability and (b) an exponential damping of the perturbation if $\frac{\partial \sigma_{eq}(\varepsilon_0,\theta_0)}{\partial \varepsilon} > 0$, which implies stability. This behavior explains the apparition of local dynamic effects and indicates that the inertial terms in the balance of momentum cannot be a priori neglected even for very low quasi-static tests.

For the piecewise linear thermoelastic model (2)–(4), the free energy $\psi_{mx} = \psi_{mx}(\varepsilon, \sigma, \theta)$ can be explicitly calculated, according to the formulas in ▶ Maxwellian Rate-Type Thermo-viscoelastic Bar Theory (see also [3]), and used to solve numerically some initial-boundary value problems for the system (7)–(10). Besides the above-mentioned input data, we use the following numerical entries: $E = 31.5$ GPa, $\kappa = 20\,\mathrm{W/m/^{\circ}K}$, $L = 20\,\mathrm{mm}$, and $R = 2\,\mathrm{mm}$. Let us note that the dynamic Young modulus E satisfies the subcharacteristic condition.

The numerical solution is obtained by using a first-order accuracy fractional-step method (see [11, Chap. 7]). One splits the system (7)–(10) with source terms into two subproblems. In a first step one considers the hyperbolic homogeneous part of the system, and one uses a first-order characteristic method for the characteristic directions $\pm\sqrt{E/\varrho}$. In a second step, one considers a simple ordinary differential equation system containing the source terms which depends on θ_{XX}, too. The time integration step must be of the order of the relaxation time $\frac{\mu}{E}$, that is, one should not step to fast in time in order to give to the viscous effects enough time to develop.

To investigate the predictions of the Maxwellian model, it is useful to simulate the following two laboratory experiments.

Quasi-Static Strain-Controlled Test: Pseudoelastic Behavior

One considers a bar initially at rest, unstressed, at the uniform temperature $\theta_0 = 36.7^{\circ}\mathrm{C}$ in the $\mathcal{A}$ phase. The environmental temperature is all the time constant and equal with the initial temperature, that is, $\theta_{ext}(t) = \theta_0$ for any $t > 0$. The bar ends satisfy isothermal conditions, that is, $\theta(0,t) = \theta_0$ and $\theta(L,t) = \theta_0$ for any $t > 0$. The right end of the bar is fixed while the left end is pulled with a constant velocity until the transformation is complete, that is, $v(0,t) = V^* = L\,\dot{\varepsilon}_e = \text{const.} < 0$ and $v(L,t) = 0$ for $t \in [0, t_1]$.

The strain-controlled experiment illustrated in Figs. 4–6 corresponds to a quasi-static test where $\dot{\varepsilon}_e = 5 \times 10^{-3}/\mathrm{s}$. The bar is supposed to be in an air-like convective medium, that is, $\omega = 20\,\mathrm{W/m^2/^{\circ}K}$, and the relaxation time of the model is $\frac{\mu}{E} = 10^{-4}\,\mathrm{s}$.

If one represents the stress $\sigma(0,t)$ versus the engineering strain $\varepsilon_e(t) = \frac{1}{L}\int_0^L \varepsilon(X,t)\mathrm{d}X$, one gets a linear stress-strain relation with the slope E_1 as long as the bar is homogeneous in the stable phase $\mathcal{A}$. For this part of the deformation process, the material response is practically

thermoelastic. Because μ is very small, the viscous effect is unnoticed. The role of the viscosity (relaxation time) becomes extremely important when particles of the bar enter in the unstable region $\mathcal{I}^+$. One observes that each nucleation of martensite and front-phase propagation is accompanied by a stress drop. This behavior results in a sawtooth stress-strain curve which characterizes the $\mathcal{A} \rightarrow \mathcal{M}^+$ phase transformation process of the bar (Fig. 4a). The typical features of a tooth are illustrated in Fig. 4b.

There is a first stage marked with labels ① and ② which corresponds to the nucleation of the new phase. One sees in Fig. 5 how the strain starts to develop and the local temperature to increase. The second stage, which is represented by ③, is just the abrupt stress drop when the strain localization occurs very rapidly. It is a *local dynamic event* during which the particles which undergo the phase transformation cross the region $\mathcal{I}^+$. This behavior illustrates why the inertial term in the balance of momentum (7) cannot be neglected even in a quasi-static test. The phase transformation process is accompanied by a significant localized increase of the temperature (around 3°C). The third stage, represented by labels ④ and ⑤, corresponds to an ascending branch of the stress-engineering strain curve with a slope between E_1 and E_3. This part corresponds to a quasi-static process along which the strain distribution in the bar remains unchanged, that is, the phase fronts are arrested. Only the peaks of temperature decay due to the axial heat diffusion (Fig. 5). The phase transformation process is thus of the type "go-and-stop" strain band propagation. The amplitude of the serrations depends on the size of the time of relaxation, that is, on μ, and on the imposed strain rate $\dot{\varepsilon}_e$ (see [3]). These numerical results prove a good agreement with the full-field measurements of strain and temperature and their correlation with the stress-engineering strain curve obtained in [9] for strain-controlled experiments.

An overview of the $\mathcal{A} \rightarrow \mathcal{M}^+$ phase transformation process is illustrated in Fig. 6a. For the strain rate considered here, the heat transfer to the environment cannot keep up with the rate at which latent heat is released by the material. Thus, one can observe that as the fronts propagate, the hot zones spread and the local temperatures increase.

Once the transformation is complete, after a relaxation process in the martensite phase $\mathcal{M}^+$, the specimen recovers the ambient temperature and the stress decays with 4 MPa. It is worth to note that this stress relaxation is not due to the viscosity of the model but to the decay of the temperature of the bar and to the fact that $\frac{\partial \sigma_{eq}}{\partial \theta}$ is negative in this region. That means it is not a viscoelastic behavior.

If one starts an unloading process at constant strain rate, one gets a linear stress-strain behavior with the elastic modulus E_3 of the $\mathcal{M}^+$ phase. The unstable transformation occurs through serrations characterized by a sudden increase of the stress as the $\mathcal{A}$ phase nucleates and propagates at the expense of $\mathcal{M}^+$ phase. This behavior is accompanied by a local decrease of the temperature of the transformed zone. This local dynamic event is followed by a quasi-static process during which the stress decreases with a positive stress-strain slope. An overall view is illustrated in Fig. 6a. Let us note how the temperature of the specimen becomes progressively colder.

Temperature-Controlled Test: Shape Memory Effect

We consider the bar initially at rest, unstressed, in the A phase, at the temperature $\theta_0 > \theta_m$ such that $\sigma_m(\theta_0)<0$. This choice allows the coexistence at this temperature of the $\mathcal{A}$ phase and $\mathcal{M}^+$ phase in a free-stress state (see Fig. 1a). Maintaining a constant ambient temperature equal to the initial temperature $\theta_0 = 11.8°\mathrm{C}$, the bar firmly fixed at one end, is subjected to a traction test, with the constant strain rate $\dot{\varepsilon}_e = 5 \times 10^{-3}/\mathrm{s}$ until the transformation is complete. It is followed by an unloading stress-controlled test until the load is completely removed, and the bar remains largely deformed in the $\mathcal{M}^+$ phase. The bar has been supposed to be in a water-like convective medium, that is, $\omega = 1000\ \mathrm{W/m^2/°K}$, and the relaxation time is $\frac{\mu}{E} = 10^{-3}\ \mathrm{s}$. One gets the stress-engineering

strain curve illustrated in Fig. 7a and a self-heating of the bar during the $\mathcal{A} \to \mathcal{M}^+$ transformation as described previously.

After the specimen in $\mathcal{M}^+$ phase recovers the initial temperature, one simulates the shape memory effect. One increases the ambient temperature with a constant temperature rate, that is, $\theta_{ext}(t) = \dot{\theta}_e\, t + \theta_0$, where $\dot{\theta}_e = 1^\circ\mathrm{C}/s$ for $t > 0$. One end of the bar is fixed and the other verifies a free-stress end condition. In order to have the same type of heat transfer condition at the ends of the specimen and across its lateral surface, one considers the following boundary conditions: $-\kappa\frac{\partial\theta}{\partial X}(0,t) = -\omega(\theta(0,t) - \theta_{ext}(t))$ and $-\kappa\frac{\partial\theta}{\partial X}(L,t) = -\omega(\theta(L,t) - \theta_{ext}(t))$ for $t > 0$.

The predictions of the Maxwellian rate-type model for a temperature-induced phase transformation are illustrated in Figs. 7b and 8. By increasing the external temperature, one increases in a homogeneous way the temperature of the bar lying in the stable phase $\mathcal{M}^+$. The deformation field remains almost unchanged and homogeneous, satisfying conditions $\varepsilon(X,t) \geq \varepsilon_m(\theta(X,t))$ and $\sigma(X,t) \approx \sigma_{eq}(\varepsilon(X,t), \theta(X,t)) \approx 0$. Due to the increase of temperature, the equilibrium stress $\sigma = \sigma_{eq}(\varepsilon, \theta)$ moves upward, and one arrives at a time t when a particle X of the bar enters the unstable region $\mathcal{I}^+$, that is, $\varepsilon(X,t) < \varepsilon_m(\theta(X,t))$, and the stress $\sigma(X,t)$ equals the minimum stress $\sigma_m(\theta(X,t))$ which becomes positive. In this situation the only equilibrium free-stress alternative belongs to the $\mathcal{A}$ phase, and the bar snaps back to its original dimension. The small circles on the graph in Fig. 7a correspond to the small circles in Fig. 7b, giving an image on the way the bar shrinks by smooth steps.

Figure 8a illustrates that the Maxwellian rate-type model can describe the nucleation events as well as the unstable and inhomogeneous character of the strain field during the temperature-induced $\mathcal{M}^+ \to \mathcal{A}$ phase transformation which leads to the recovery of the initial dimension of the bar. Moreover, this approach can capture the competition between the external heating of the bar and the endothermic character of the reverse $\mathcal{M}^+ \to \mathcal{A}$ transformation. Thus, Fig. 8b clearly illustrates that although one continuously heats the specimen, the transformed zones are accompanied by local temperature drops.

Cross-References

- Maxwellian Rate-Type Thermo-Viscoelastic Bar Theory: An Approach to Non-monotone Thermoelasticity
- Thermoelastic Bar Theory

References

1. Lagoudas DC (ed) (2008) Shape memory alloys. Modeling and engineering applications. Springer, New York/London
2. Făciu C, Suliciu I (1994) A maxwellian model for pseudoelastic materials. Scripta Metall Mater 31:1399–1404
3. Făciu C, Mihăilescu-Suliciu M (2002) On modelling phase propagation in SMAs by a Maxwellian thermo-viscoelastic approach. Int J Solids Struct 39:3811–3830
4. Abeyaratne R, Kim SJ, Knowles JK (1994) A one-dimensional continuum model for shape memory alloys. Int J Solids Struct 31:2229–2249
5. Otsuka K, Wayman CM (eds) (1998) Shape memory materials. Cambridge University Press, Cambridge
6. Abeyaratne R, Knowles JK (2006) Evolution of phase transformation. A continuum theory. Cambridge University Press, Cambridge, New York
7. Ericksen JL (1975) Equilibrium of bars. J Elast 5:191–201
8. Shaw JA (2000) Simulations of localized thermo-mechanical behavior in a NiTi shape memory alloy. Int J Plast 16:541–562
9. Shaw JA, Kyriakides S (1997) On the nucleation and propagation of phase transformation fronts in a NiTi alloy. Acta Mater 45:683–700
10. Făciu C, Molinari A (2006) On the longitudinal impact of two phase transforming bars. Elastic versus a rate-type approach. Part I: The elastic case. Part II: The rate-type case. Int J Solids Struct 43:497–522, 523–550
11. LeFloch PG (2002) Hyperbolic systems of conservation laws. The theory of classical and nonclassical shock waves. Birkhäuser, Basel/Boston/Berlin
12. Făciu C, Mihăilescu-Suliciu M (2005) Shape memory effect: a Maxwellian rate-type constitutive approach. In: Mihăilescu-Suliciu M (ed) New trends in continuum mechanics. Theta Publisher, Bucharest, pp 139–145

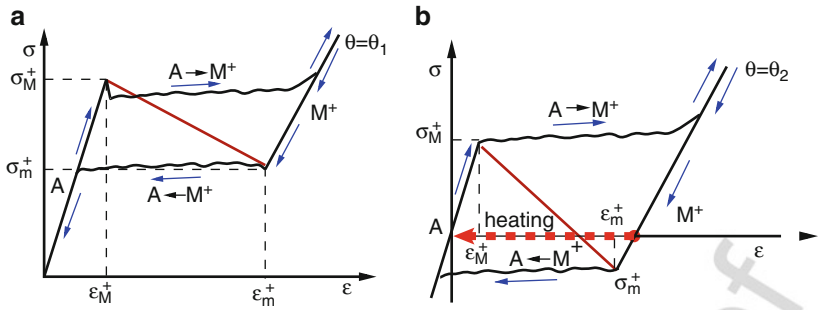

Pseudoelasticity and Shape Memory Effect: A Maxwellian Rate-Type Approach, Fig. 1 Illustrative quasi-static stress-strain curves for thin SMA bars at two representative temperatures $\theta_1 > \theta_2$. (**a**) Hysteretic behavior at temperature θ_1. (**b**) Hysteretic behavior at temperature θ_2. Loading, unloading, and restoring the initial shape by heating at the free-stress state

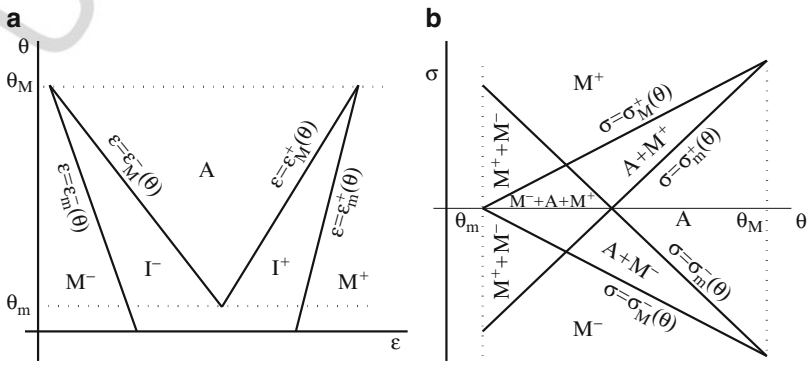

Pseudoelasticity and Shape Memory Effect: A Maxwellian Rate-Type Approach, Fig. 2 Phase diagrams: (**a**) austenite $\mathcal{A}$, martensite $\mathcal{M}^{\pm}$, and unstable $\mathcal{I}^{\pm}$ regions in the (ε, θ) plane; (**b**) available phases at a given state (σ, θ)

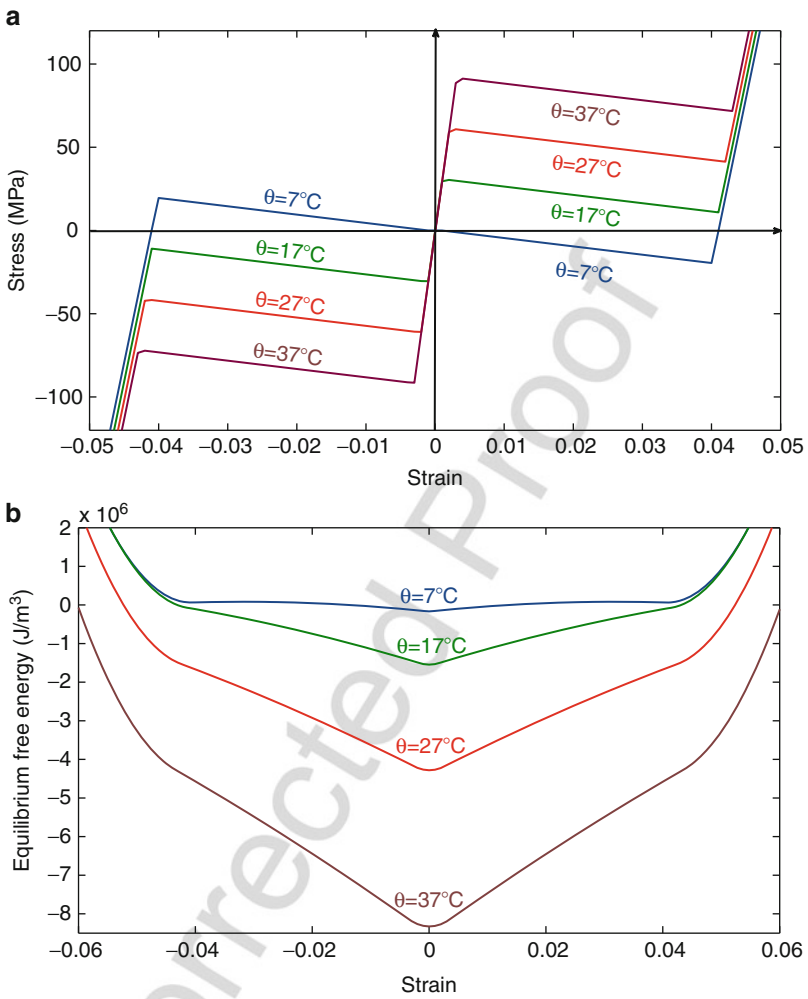

Pseudoelasticity and Shape Memory Effect: A Maxwellian Rate-Type Approach, Fig. 3 (**a**) Non-monotone equilibrium stress-strain relations described by (2) for different temperatures and (**b**) the corresponding non-convex free energy functions $\psi = \psi_{eq}(\varepsilon,\ \theta)$

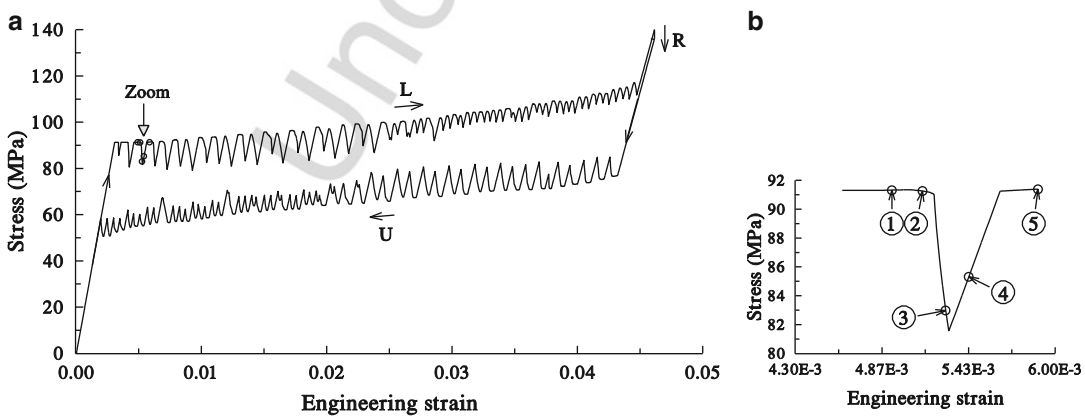

Pseudoelasticity and Shape Memory Effect: A Maxwellian Rate-Type Approach, Fig. 4 (**a**) Unstable pseudoelastic behavior in a strain-controlled experiment at $\dot{\varepsilon}_e = \pm 5 \times 10^{-3}$. (**b**) Zoom of the third stress drop (From [3])

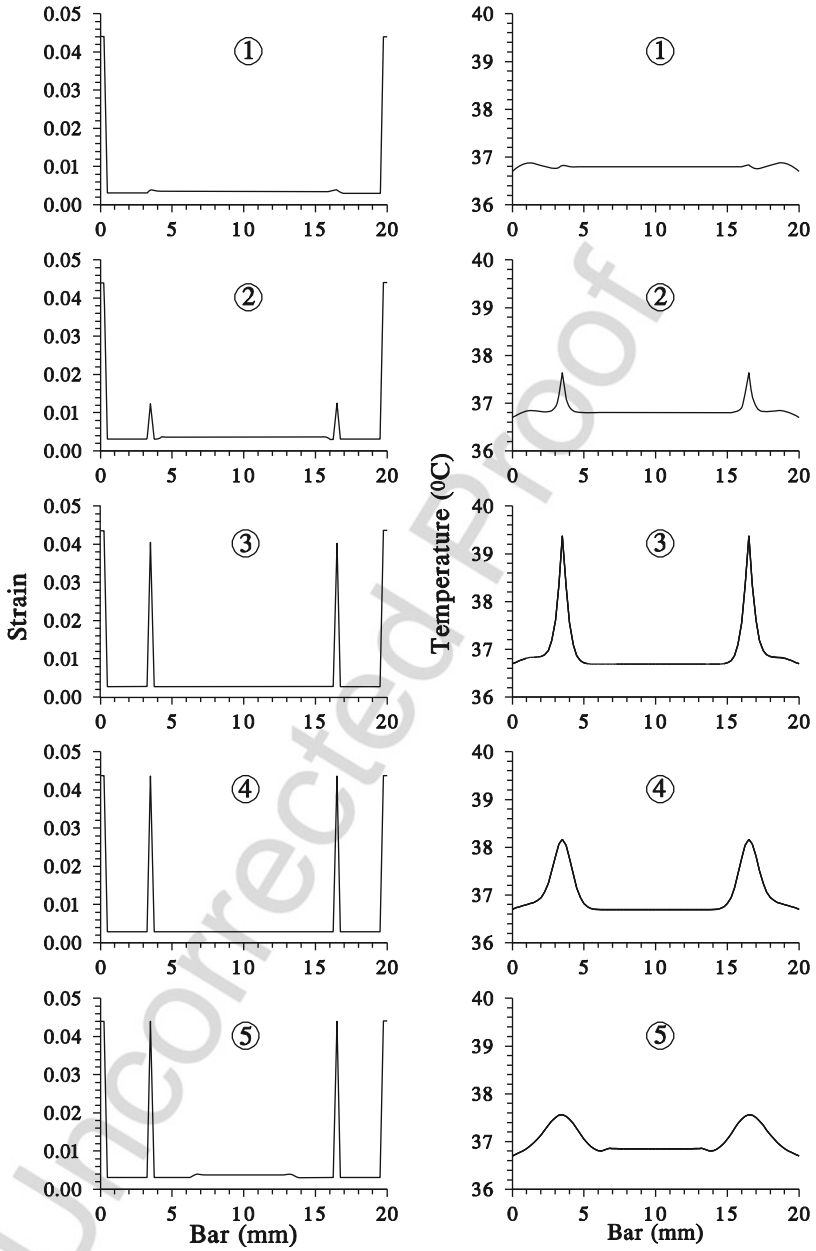

Pseudoelasticity and Shape Memory Effect: A Maxwellian Rate-Type Approach, Fig. 5 Strain and temperature distribution in the bar corresponding to the labeled positions in the zoom in Fig. 4a – nucleation and localization of strain during $\mathcal{A} \rightarrow \mathcal{M}^{+}$ phase transformation (From [3])

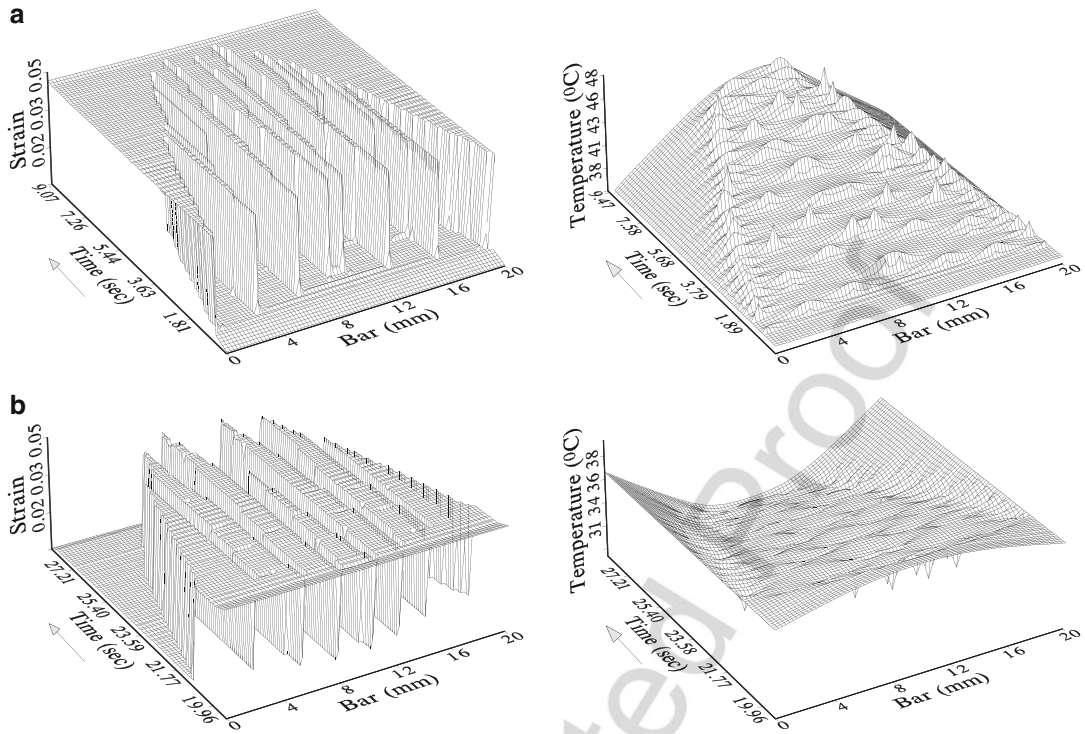

Pseudoelasticity and Shape Memory Effect: A Maxwellian Rate-Type Approach, Fig. 6 Strain and temperature evolution in the bar during pseudoelastic hysteresis in Fig. 4. (**a**) During *loading*: *self-heating* of the bar and unstable and inhomogeneous $\mathcal{A} \to \mathcal{M}^+$ phase transformation; (**b**) during *unloading*: *self-cooling* of the bar and unstable and inhomogeneous reverse $\mathcal{M}^+ \to \mathcal{A}$ phase transformation (From [3])

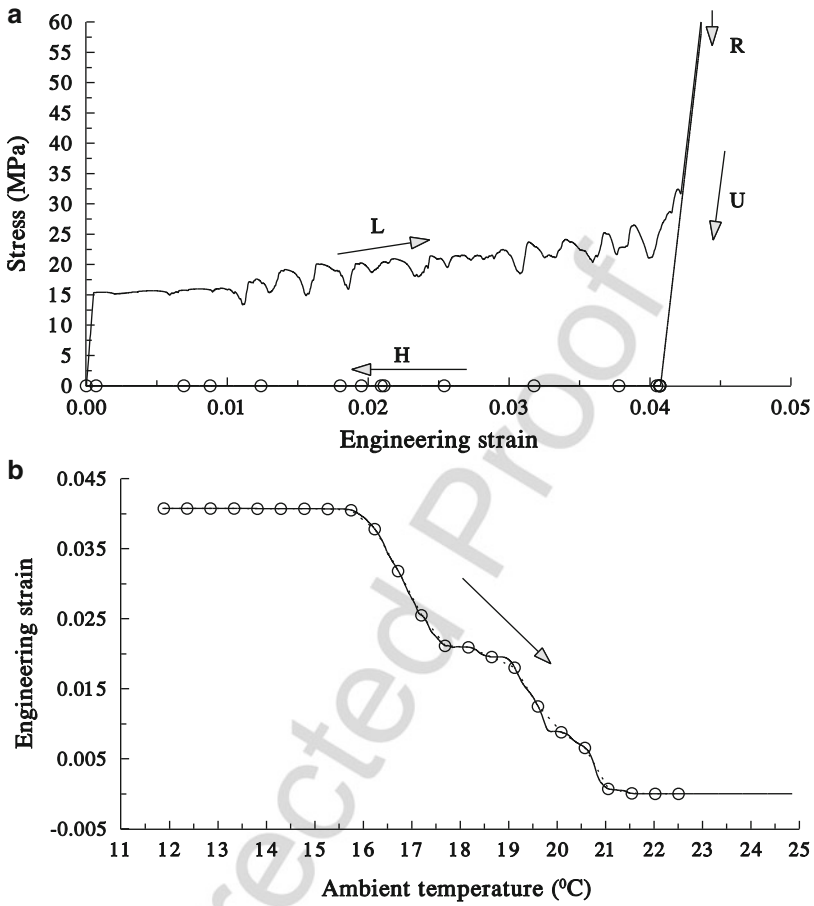

Pseudoelasticity and Shape Memory Effect: A Maxwellian Rate-Type Approach, Fig. 7 Shape memory effect: (**a**) loading, relaxation, unloading, and external heating of the bar; (**b**) evolution of the engineering strain during heating of the unstressed bar ($\dot{\theta}_e = 1°\mathrm{C/s}$) (From [12])

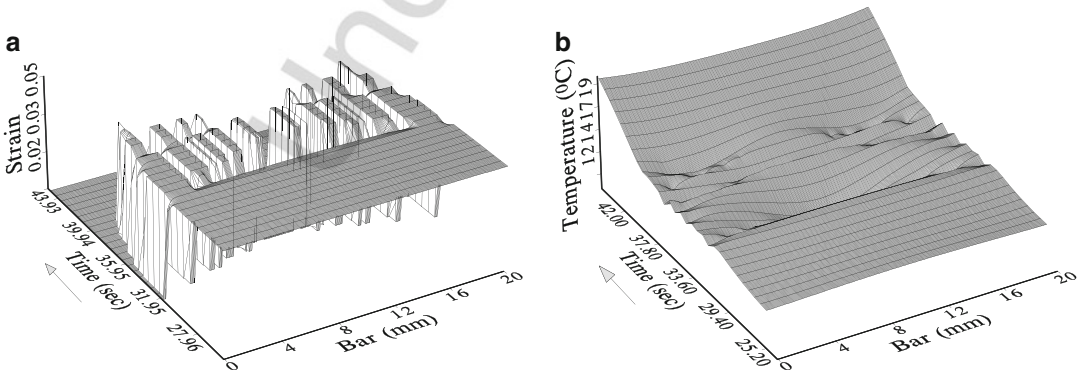

Pseudoelasticity and Shape Memory Effect: A Maxwellian Rate-Type Approach, Fig. 8 Shape memory effect – strain and temperature field evolution in the unstressed bar during heating of the external environment of the bar, $\theta_{ext}(t) = 11.8°\mathrm{C} + \dot{\theta}_e\, t$ (From [12])